TECHNICAL ARTICLE

Neutron diffraction residual stress measurements of welds made with pulsed tandem gas metal arc welding (PT-GMAW)

A.M. Paradowska,[1] N. Larkin,[2] H. Li,[2] Z. Pan,[2] C. Shen,[2] and M. Law[1,a)]
[1]Australian Nuclear Science and Technology Organisation (ANSTO), New Illawarra Rd, Lucas Heights, NSW 2234, Australia
[2]University of Wollongong, Northfields Ave, Wollongong, NSW 2522, Australia

(Received 8 September 2014; accepted 30 September 2014)

Pulsed tandem gas metal arc welding (PT-GMAW) is being developed to increase productivity and minimise weld-induced distortion in ship-building. The PT-GMAW process was used in pulse–pulse mode to butt-weld two different strength and thickness steels; the residual stress and hardness profiles of the welds are reported and correlated. © *2014 International Centre for Diffraction Data.*
[doi:10.1017/S0885715614000992]

Key words: Residual stress, distortion, welding

I. INTRODUCTION

Welding residual stresses are primarily owing to the differences in temperature distribution in the weld and parent metal during heating and cooling cycles (Withers and Bhadeshia, 2001). These thermally induced stresses can exceed yield and cause strain misfit on cooling. Residual stresses can lead to fracture, reduced fatigue life, and stress corrosion cracking (Webster and Wimpory, 2001). Residual stress can also lead to hydrogen cracking and distortion, which are significant problems in shipbuilding; the cost of correcting weld distortion in shipbuilding may be up to 30% of the fabrication costs (Andritsos and Perez-Prat, 2000). Welding distortion is affected by many factors, including component design, welding sequence, and heat input, with the most important factor being the level of residual stress. Residual stresses may cause hydrogen cracking of welds in the presence of trapped hydrogen and a susceptible microstructure, often defined as a microstructure with a hardness value of more than 350 HV (API Standard 1104, 2005; CSA-Z662, 2007). Microstructures with high hardness values are caused by the same high temperatures which cause residual stresses, with the addition of fast cooling rates. Hydrogen content can be controlled by electrode choice and welding procedure.

Neutron diffraction (ND) can be used to obtain residual stresses non-destructively with high spatial resolution of ≤1 mm to a depth of many millimetres below the weld surface (up to 50 mm for steel). ND been successfully applied to evaluate residual stresses in many welded components (Law *et al.*, 2010; Paradowska *et al.*, 2010a, 2010b; Assuncao *et al.*, 2011; Law and Luzin, 2011; Suder *et al.*, 2011).

The pulsed tandem gas metal arc welding (PT-GMAW) process promises to: (1) deliver high deposition rates; (2) perform out-of-position welding; and (3) achieve low levels of weld distortion (Yudobidroto *et al.*, 2006). Residual stresses have not been previously measured in PT-GMAW welds, and this experiment aims to investigate, using ND, the hardness and residual stress profiles of welds made by PT-GMAW.

a)Author to whom correspondence should be addressed. Electronic mail: mlx@ansto.gov.au

II. EXPERIMENTAL

A. Samples

The samples were DH36 steel plates 4.5 mm thick × 200 mm wide × 300 mm long, and HSLA65 steel plates of 8 × 150 × 285 mm^3. Welds were made along the whole length, in full penetration mode. Both samples were made by PT-GMAW, which used a ceramic backing and a Fronius PT-GMAW system in pulse–pulse mode, a shielding gas of 16.5% CO_2, 1.5% O_2, and 82% Ar flowing at 30 l min^{-1}, a torch angle of 10° (push), a wire feed speed of 12–16 m min^{-1}, and a travel speed of 750 mm min^{-1}.

B. Hardness testing

Hardness testing was performed across the weld with a Leco micro hardness testing machine with an indentation mass of 1 kg. The HSLA65 weld is harder than the DH36 weld in every zone (Figure 1). In both the materials, the heat-affected zone is hardest, followed by the weld, and then the parent material, with the differences being greater in the HSLA65 material. No hardness values are above 350 HV, which is where hydrogen cracking is likely to occur.

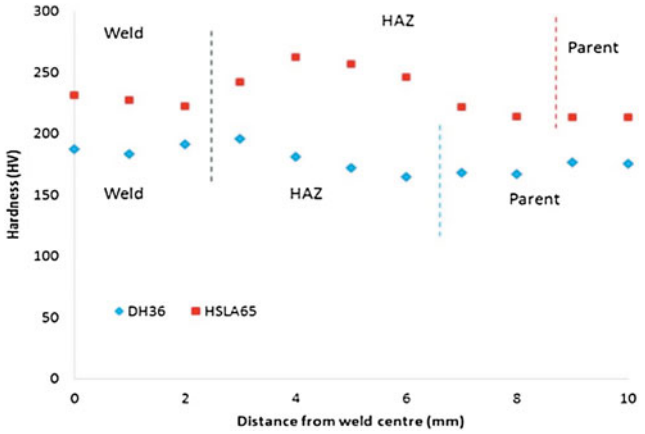

Figure 1. (Color online) Hardness traverse of DH36 and HSLA65 welds.

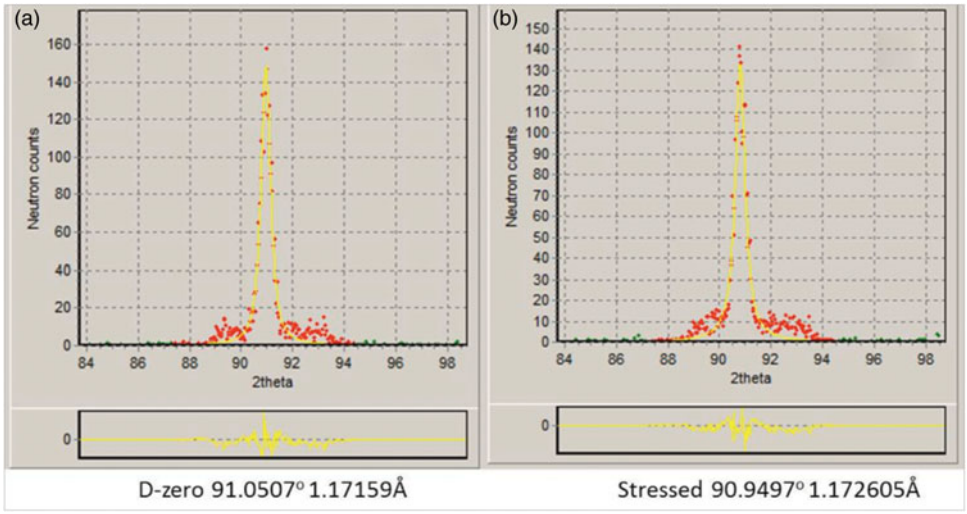

Figure 2. (Color online) Peak shift between unstressed (a) and stressed (b) gauge volumes, indicating a strain of 867 microstrain.

C. Neutron residual stress measurements

Knowing the neutron wavelength (λ) and the Bragg scattering angle (θ), and the inter-planar spacing (d) can be calculated via the Bragg equation. If the inter-planar spacing (d_0) of an unstressed sample is also known (Figure 2), the elastic strain in the scattering vector direction can be calculated *via*

$$\varepsilon = \frac{d}{d_0} - 1 \tag{1}$$

When the strains in a number of directions are known the full stress field can be calculated (Hutchings and Krawitz, 1992; Hutchings *et al.*, 2005). The simplest solution is when the strains are measured in the same direction as the three principal stresses, then

$$\sigma_1 = \frac{E}{(1+\nu)(1-2\nu)}((1-\nu)\varepsilon_1 + \nu(\varepsilon_1 + \varepsilon_1 + \varepsilon_1)) \tag{2}$$

The example shown in Figure 2 shows a peak shift of $0.101°2\theta$, which indicates a strain of 867 microstrain. In a uniaxial stress state, this would be equivalent to a stress of 173 MPa, but the actual value in a component depends on the other two strains.

Through-thickness scans were performed on the weld and parent material (Figure 3) in three directions orthogonal to the plate axes, which were assumed to be the same as the principal stress directions. The longitudinal stress is aligned with the weld direction, the transverse stress is cross-weld, and the normal stress is through-thickness.

The residual stress measurements were performed on the Kowari strain scanning instrument at the OPAL research reactor at the Australian Nuclear Science and Technology Organisation (ANSTO). A monochromatic beam of $\lambda = 1.672$ Å was chosen, so that the Fe (211) scattering planes in the sample resulted in a scattering angle close to 90°, which reduces many possible geometric errors in measurement (Hutchings *et al.*, 2005). A nominal gauge volume of $1 \times 1 \times 1$ mm^3 was used. Each sample was measured at three through-thickness positions, 1 mm below each surface and in the middle of the thickness. Since the composition and microstructure vary across the weld and parent material, stress free (d_0) lattice spacing values were made for each measurement point. To calculate the stresses from the strains, values for Young's modulus (E) of 207 GPa and Poisson's ratio (ν) of 0.3 were used for both steels.

D. Residual stress results

The residual stress maps for the welded plates are shown in Figure 4. The residual stress profiles across the weld of the plates 1 mm below the surface are shown in Figure 5. The residual stress has been compared with the minimum yield strength for each steel grade.

In both welds, the residual stress in the along-weld direction (longitudinal) was highest. The normal direction residual stress for DH36 was compressive or close to zero across the weld, and transverse residual stresses were highest in the vicinity of the weld. The residual stresses in the DH36 material were lower, and also had a lower gradient between the parent and weld, both of which will reduce distortion. For the HSLA65 weld, transverse residual stresses were higher on either side of the weld. Normal direction residual stresses (through-thickness) were compressive in the vicinity of the weld, and close to zero outside of the weld.

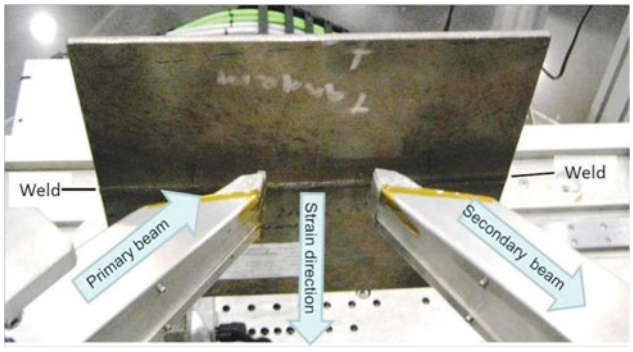

Figure 3. (Color online) Welded sample during measurement on the Kowari instrument. The primary beam comes from the monochromator; the secondary beam is the diffracted neutrons. The measured strain direction lies between these two beams.

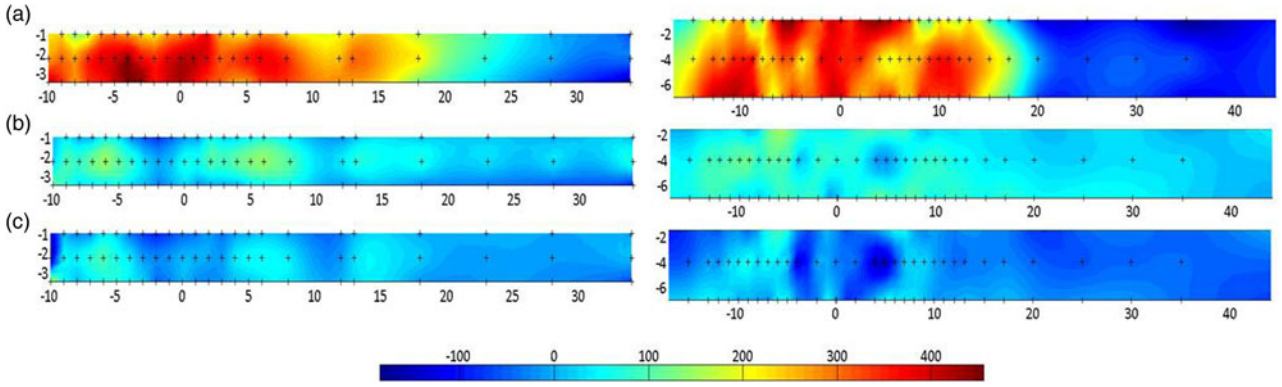

Figure 4. (Color online) Residual stress profile through-thickness of the DH36 4.5 mm plate (left) and HSLA65 8 mm plate (right). Longitudinal stresses (a), transverse stress (b), and normal stresses (c).

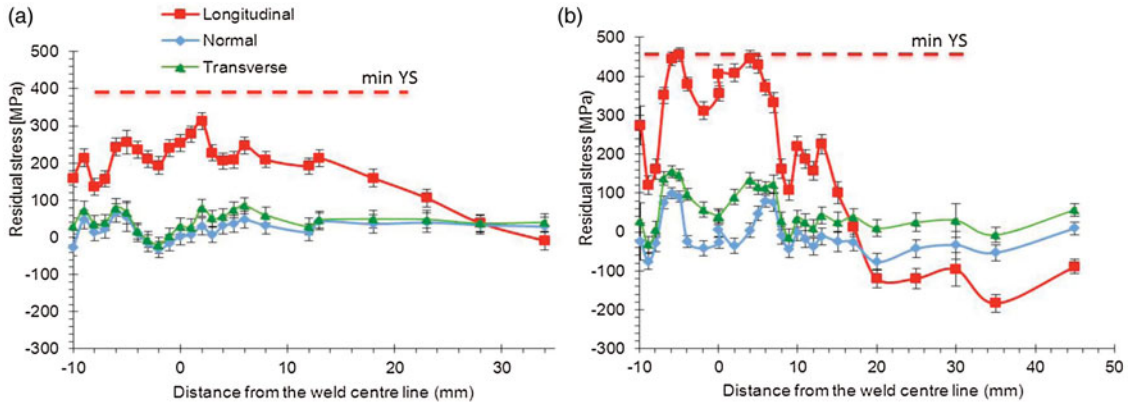

Figure 5. (Color online) Residual stress profile: (a) 1 mm below the surface across the DH36 4.5 mm welded plate, and (b) the HSLA65 8 mm welded plate.

E. Comparison of hardness and residual stress results

The hardness of the DH36 shows a slow decline from the weld toward the parent metal (Figure 1), and the residual stress profile for this steel shows the same trend (Figure 5). The highest residual stresses and hardness were both found in the HSLA65 weld, reflecting the higher yield strength of the weld material. Although the highest hardness values are below the 350 HV limit for hydrogen cracking, the coincidence of these with the position of highest residual stresses demonstrates the potential for hydrogen cracking if the welding procedure is not adhered to.

III. CONCLUSION

Detailed residual stress and hardness distributions were presented for welds made by PT-GMAW on DH36 and HSLA65 steels. In both materials, the highest stresses were found in the weld material and lie in the weld direction. These were balanced by lesser compressive residual stresses in the parent material. The cross-weld stresses are self-balancing and are highest in the crown of the weld. Transverse residual stresses were found to be highest in the middle thickness of the plate in both welds. The HSLA 65 welded plate had the highest residual stresses. The position of highest hardness values corresponds to the position of highest residual stress. The DH36 material's residual stress distribution will lead to less distortion.

Andritsos, F. and Perez-Prat, J. (**2000**). *The Automation and Integration of Production Processes in Shipbuilding* (Joint Research Center, European Commission, Ispra, Italy).

API Standard 1104 (**2005**). *Welding of Pipelines and Related Facilities* (American Petroleum Institute, Washington, DC), 20th ed.

Assuncao, E., Yapp, D., Suder, W., Ganguly, S., Williams, S., and Paradowska, A. M. (**2011**). "Characterisation of residual stress state in laser welded low carbon mild steel plates produced in keyhole and conduction mode," Sci. Technol. Weld. Joining **16**, 239–243.

CSA Z662-07 (**2007**). *Oil and Gas Pipeline Systems* (CSA International, Canada).

Hutchings, M. T. and Krawitz, A. D. (eds) (**1992**). *Measurement of Residual and Applied Stress Using Neutron Diffraction*, NATO ASI Series 216E (Kluwer Academic Publishers, Dordrecht).

Hutchings, M. T., Withers, P. J., Holden, T. M. and Lorentzen, T. (**2005**). *Introduction to the Characterization of Residual Stress by Neutron Diffraction* (Taylor and Francis Publishers, Boca Raton, Florida, USA).

Law, M. and Luzin, V. (**2011**). "Effect of spatial variation of stress-free lattice spacings on measured residual stresses," J. Strain Anal. Eng. Des. **46**, 837–841.

Law, M., Kirstein, O. and Luzin, V. (**2010**). "An assessment of the effect of cutting welded samples on residual stress measurements by chill modeling," J. Strain Anal. Eng. Des. **45**, 567–573.

Paradowska, A. M., Price, J. W. H., Finlayson, T. R., Lienert, U., and Ibrahim, R. (**2010a**). "Comparison of neutron and synchrotron diffraction measurements of residual stress in bead-on-plate weldments", J. Press. Vessel Technol. **132**, 011502.

Paradowska, A. M., Price, J. W. H., Finlayson, T. R., Rogge, R. B., Donaberger, R. L., Blevins, R., and Ibrahim, R. (**2010b**). "Comparison of neutron diffraction residual stress measurements of steel butt welds with current fitness-for-purpose assessments," J. Press. Vessel Technol. **132**, 051503.

Suder, W., Ganguly, S., Williams, S., Paradowska, A. M., and Colegrove, P. (**2011**). "Comparison of joining efficiency and residual stresses in laser and laser hybrid welding," Sci. Technol. Weld. Joining **16**, 224–228.

Webster, G. A. and Wimpory, R. C. (**2001**). "Residual stress in weldments," J. Neutron Res. **9**, 281–287.

Withers, P. J. and Bhadeshia, H. K. D. H. (**2001**). "Residual stress. Part 1 – Measurement techniques," Mater. Sci. Technol. **17**, 355–365.

Yudobidroto, B. Y. B., Hermans, M. J. M., and Richardson, I. M. (**2006**). *The Influence of Pulse Synchronisation on the Process Stability During Tandem Wire Arc Welding (IIW Doc. No. XII-1910-06)*. (International Institute of Welding, Villepinte, France).